

Field evaluation and optimization of a lightweight lidar-based UAV navigation system for dense boreal forest environments

Aleksi Karhunen¹, Teemu Hakala¹, Väinö Karjalainen¹ and Eija Honkavaara¹

¹Finnish Geospatial Research Institute in National Land Survey of Finland, Vuorimiehentie 5, 02150 Espoo, Finland

Corresponding author: Aleksi Karhunen (email: aleksi.karhunen@maanmittauslaitos.fi).

This work has been submitted to the IEEE for possible publication. Copyright may be transferred without notice, after which this version may no longer be accessible.

This research was funded by the Research Council of Finland within project "DRONE4TREE - Autonomous drone solutions for single tree-based forest management" (decision no. 359404). This study has been performed with affiliation to the Research Council of Finland Flagship Forest-Human-Machine Interplay—Building Resilience, Re-defining Value Networks and Enabling Meaningful Experiences (UNITE) (decision no. 357908).

ABSTRACT The interest in the usage of uncrewed aerial vehicles (UAVs) for forest applications has increased in recent years. While above-canopy flight has reached a high level of autonomy, navigating under-canopy remains a significant challenge. The use of autonomous UAVs could reduce the burden of data collection, which has motivated the development of numerous solutions for under-canopy autonomous flight. However, the experiments conducted in the literature and their reporting lack rigor. Very rarely, the density and the difficulty of the test forests are reported, or multiple flights are flown, and the success rate of those flights is reported. The aim of this study was to implement an autonomously flying quadrotor based on a lightweight lidar using openly available algorithms and test its behavior in real forest environments. A set of rigorous experiments was conducted with a quadrotor prototype utilizing the IPC path planner and LTA-OM SLAM algorithm. Based on the results of the first 33 flights, the original system was further enhanced. With the optimized system, 60 flights were performed, resulting in a total of 93 test flights. The optimized system performed significantly better in terms of reliability and flight mission completion times, achieving success rates of 12/15 in a medium-density forest and 15/15 in a dense forest, at a target flight velocity of 1 m/s. At a target flight velocity of 2 m/s, it had a success rate of 12/15 and 5/15, respectively. Furthermore, a standardized testing setup and evaluation criteria were proposed, enabling consistent performance comparisons of autonomous under-canopy UAV systems, enhancing reproducibility, guiding system improvements, and accelerating progress in forest robotics.

INDEX TERMS Autonomous flying, Field experiments, Forest, Lidar, Path planning, Simultaneous localization and mapping, UAV, Under-canopy.

I. INTRODUCTION

Uncrewed aerial vehicles (UAVs) have been extensively investigated in both academic research and commercial applications. Many autonomous UAVs rely on Global Navigation Satellite Systems (GNSS) for localization. However, GNSS-based positioning becomes unreliable in forested environments due to multipath effects and signal blockages caused by dense vegetation [1]. Additionally, UAVs must be able

to perceive their surroundings to autonomously plan safe trajectories and avoid obstacles in complex environments.

Thus, numerous solutions have been proposed for flying autonomously in a GNSS-denied environment. During recent years, most solutions use either lidar [2]–[4], or camera [5]–[8] to sense the environment and to localize the UAV. However, real-world experiments conducted inside forests are often lacking or missing completely. Either the experiments

are conducted using a simulator only [4], only indoors [7], inside only simulated forests [8], or inside real-world forests [2], [3], [5], [6] with non-extensive experiments. Several shortcomings were identified in the reporting of the system evaluations. The density or the difficulty of the forest is not reported [2], [5], [6] or is only reported for the simulation experiments [3], [8]. Moreover, the success rate of flights is rarely reported for real-world experiments. Either only a result of a single flight is reported [5], [6], multiple flights are flown but the success rate is not reported [2], or the success rate of flights is only reported for the flights conducted inside a simulation [8]. For [3], the success rate for flights was reported. However, the density of the test forest was not reported, and based on the supplementary movie S1 of [3], the test forest seemed sparse. For all these reasons, the performance of most proposed autonomous flight systems operating inside dense forests is unknown.

Thus, more extensive experiments are needed to assess the performance of autonomous flight algorithms inside dense forests. Karjalainen et al. [9], [10] have performed more extensive experiments with a vision-based system based on the autonomous flight algorithm by Zhou et al. [5]. In total, 34 flights were conducted with reported forest densities, with success rates varying from 47% in a difficult forest with the original system to 100% in a medium forest and 87.5% in a difficult forest with an improved system. To our knowledge, no such extensive testing scheme has been implemented for flying inside forests for lidar-based autonomous flight systems.

This study implemented an autonomously flying quadrotor based on a lightweight lidar using openly available algorithms. For the original system, three autonomous flight and SLAM algorithms were considered. As the autonomous flight algorithms, IPC proposed by Liu et al. [2], Kumar Robotics autonomous flight proposed by Mohta et al. [11] and improved by Liu et al. [12], and CCO-VOXEL proposed by Harithas et al. [13] were considered. As the SLAM algorithms, LTA-OM proposed by Zou et al. [14], SLOAM proposed by Chen et al. [15] and improved by Liu et al. [12], and GLIM proposed by Koide et al. [16] were considered. Based on the literature, IPC was chosen as the autonomous flight algorithm due to its ability to react quickly to fast-appearing obstacles. Although forests are mostly static obstacles, the ability to quickly react to unexpected obstacles should increase the reliability of the system, especially with higher target flight velocities. LTA-OM was chosen as the SLAM algorithm due to its best performance in the manual flight localization experiment presented in subsection II-E.

In this work, the results and analysis of 93 real-world flights flown in two forest environments of differing difficulty are presented. Based on the results and analysis of the first 33 flights, the algorithm of the original system was enhanced. The performance of the optimized system is compared against the original system with flights flown in the same locations. In addition, a proposal for a more standardized

testing scheme for flights flown inside forests is presented, defining a minimum set of environmental descriptors and flight performance metrics that should be reported when testing and validating new algorithms for autonomous flights. Adhering to these policies would significantly improve the comparability of algorithm performance based solely on the literature.

II. MATERIALS AND METHODS

A. ORIGINAL AUTONOMOUS FLIGHT SYSTEM

Two open-sourced algorithms, IPC by Liu et al. [2], responsible for path planning and control, and LTA-OM by Zou et al. [14], a SLAM algorithm responsible for localization of the quadrotor, served as the foundation for the original system. The obstacle mapping module of IPC utilizes a simplified version of ROG-Map [17], where a voxel is marked as occupied if it is hit by a lidar scan. Liu et al. introduced temporal forgetting to ROG-Map, where a voxel is marked as unoccupied if no lidar scan has hit the voxel during the forgetting threshold. A* is used to find the shortest path towards the goal, and a reference path is created by pruning away redundant nodes to generate the shortest piece-wise reference path.

Model predictive control (MPC) and the differential flatness property of quadrotors [18] are used for generating a set of control inputs for the flight control unit (FCU). In the source code of IPC provided by Liu et al., the MPC problem differs slightly from the one given in [2] and is formulated as:

$$\begin{aligned} \min_{\mathbf{u}_k} & \sum_{n=1}^N \|\mathbf{u}_{n-1}\|_{\mathbf{R}_u}^2 + \sum_{n=1}^{N-1} (\|(\mathbf{p}_{\text{ref},n} - \mathbf{p}_n)\|_{\mathbf{R}_p}^2 \\ & + \|(\mathbf{v}_{\text{ref},n} - \mathbf{v}_n)\|_{\mathbf{R}_v}^2 + \|\mathbf{a}_n\|_{\mathbf{R}_a}^2) + \|(\mathbf{p}_{\text{ref},N} - \mathbf{p}_N)\|_{\mathbf{R}_{p,N}}^2 \\ & + \|\mathbf{v}_N\|_{\mathbf{R}_{v,N}}^2 + \|\mathbf{a}_N\|_{\mathbf{R}_{a,N}}^2 + \sum_{n=0}^{N-2} \|\mathbf{u}_{n+1} - \mathbf{u}_n\|_{\mathbf{R}_c}^2 \end{aligned} \quad (1)$$

where $\|\mathbf{u}_{n-1}\|_{\mathbf{R}_u}^2$ is the control efforts, $\|(\mathbf{p}_{\text{ref},n} - \mathbf{p}_n)\|_{\mathbf{R}_p}^2 + \|(\mathbf{v}_{\text{ref},n} - \mathbf{v}_n)\|_{\mathbf{R}_v}^2 + \|\mathbf{a}_n\|_{\mathbf{R}_a}^2$ are the reference path, velocity, and acceleration following error at reference positions $[\mathbf{p}_{\text{ref},1}, \dots, \mathbf{p}_{\text{ref},N-1}]$ respectively, $\|(\mathbf{p}_{\text{ref},N} - \mathbf{p}_N)\|_{\mathbf{R}_{p,N}}^2 + \|\mathbf{v}_N\|_{\mathbf{R}_{v,N}}^2 + \|\mathbf{a}_N\|_{\mathbf{R}_{a,N}}^2$ are the reference path, velocity, and acceleration error at the reference position of the horizon length $\mathbf{p}_{\text{ref},N}$ respectively, and $\|\mathbf{u}_{n+1} - \mathbf{u}_n\|_{\mathbf{R}_c}^2$ is the control variation. The MPC problem is practically the same as presented in [2, eq. (2a)], but with greater flexibility in parameter selection. Instead of having the same weight parameter for every position, velocity, and acceleration index, a different weight parameter can be used for the intermediate reference indexes and the last index. Two safe flight corridors (SFCs) [19] are used as the safe space constraint for the MPC problem. The control commands given by solving the MPC problem, given as a set of jerk commands, are transformed to a set of attitude commands by utilizing the differential flatness property [18] of quadrotors.

LTA-OM utilizes FAST-LIO2 [20] as the odometry module. STD-LCD [21] is used for detecting loop closures. LTA-OM employs a false positive rejection scheme where every loop closure candidate has to pass a consistency check before being inserted properly into the pose graph. FAST-LIO2 of LTA-OM was modified so that odometry is published at IMU rate instead of lidar rate. Between the odometry estimations from the lidar scans, the odometry estimation is forward propagated with a second-order integrator. The whole system operates on the Robot Operating System (ROS) [22].

B. OPTIMIZED AUTONOMOUS FLIGHT SYSTEM

Based on the experiments conducted with the original system, a number of modifications were implemented to the original autonomous flying algorithm.

During the flight experiments with the original system, the quadrotor flew erratically in place, especially in denser areas. Since A* always tries to find the shortest path towards the goal, when replanning is triggered, the next reference path might start in a completely different direction than the last. This led to situations where the quadrotor flew up and down or left and right, remaining in place for an extended period. A more detailed description of the behavior is presented in subsection III-A. To alleviate this problem, the path planning module is modified so that A* tries to generate a path that follows the last reference path during the replanning process. This is achieved by modifying the heuristic function of A* by adding a penalty term that penalizes the current grid node based on the distance of the node from the last reference path:

$$h(n) = \begin{cases} d(n)_{\text{goal}} + wd(n)_{\text{last_path}} & d(n)_{\text{start}} \leq d_{\text{follow}} \\ d(n)_{\text{goal}} & d(n)_{\text{start}} > d_{\text{follow}} \end{cases}, \quad (2)$$

where $d(n)_{\text{goal}}$ is the distance from the current grid node n to the goal, $d(n)_{\text{last_path}}$ is the shortest distance from n to the last reference path, $d(n)_{\text{start}}$ is the distance from n to the starting grid node of the search, d_{follow} is the distance threshold from the start inside of which the old path should be followed, and w is the weight parameter which influences how strongly the old path should be followed. Using the modified heuristic will slow down the A* search considerably if the path towards the goal is hard to find. Thus, to speed up the search in these instances, after the first node is found outside the old path following radius d_{follow} , neighbors that are located closer than 80% of d_{follow} from the start are not added to the open set. Of course, this might lead to a situation where a path is not found, even if it exists; thus, a new search is triggered without the old path following if no path is found. The A* search might sometimes take too long. Therefore, an emergency stop procedure will be activated if the path search takes longer than 0.1 seconds to complete. After the emergency stop procedure, the same A* path search is continued in chunks of 0.1 seconds until the A* search terminates.

The second modification to the system is error handling when "Not a numbers" (NaNs) are generated during the SFC generation process. If NaN errors are not handled, it will lead to MPC generating control inputs with NaNs, which will cause the PX4 FCU, which was used as the FCU of the system, to shut down the engines. In the optimized system, an emergency stop procedure is activated where all MPC target positions are set to the current position, all MPC goal velocity and acceleration targets are set to zero, and the SFC is set as the default bounding box as described in [19].

Lastly, the direction of gravity is measured before takeoff by taking 200 IMU measurements and taking the average direction of acceleration as the direction of gravity. This allows the quadrotor to plan paths that are perpendicular to the direction of gravity, even when the starting location is on a slope. Without the gravity alignment of the initial pose, the height estimation will be erroneous when starting the flight from a slope.

C. HARDWARE

The real-world experiments were conducted with a custom-built quadrotor. The onboard computer was a Minisforum EM780 (Minisforum, Hong Kong, China) with AMD Ryzen 7 7840U (AMD, Santa Clara, CA, USA) CPU. Pixhawk 6C mini (Holybro, Hong Kong, China) was used as the PX4-compliant FCU, which was responsible for control of the quadrotor given the attitude commands generated by the MPC module. Livox Mid-360 Lidar (Livox Technology, Shenzhen, China) was selected as the lidar for the system. It is a lightweight and small lidar, weighing only 265 grams, with an exterior measure of 65×65×60 mm, which enables the whole system to be similar in weight and size to stereo camera-based quadrotors. It outputs 200,000 points a second in a non-repeating manner, and the field of view of the lidar is 360° horizontally, 7° downwards, and 52° upwards. The built-in IMU of the Livox Mid-360, ICM40609, was employed as the IMU of the system. The output rate of the lidar was set to 10 Hz, and the output rate of the IMU was 200 Hz.

The hardware was mounted to a frame with a motor-to-motor distance of 350 mm. The prop length of the two-bladed propellers was 17.8 cm (8 inches). The weight of the platform was 1245 grams without the battery and 1875 grams with the 10 Ah battery. The quadrotor platform is shown in Figure 1.

D. TEST ENVIRONMENTS AND EXPERIMENTAL SETUP

The performance of both the original and optimized systems was evaluated in two boreal forest areas located in Paloheinä, Helsinki (60°15'28.4"N 24°55'19.9"E). Based on forest complexity, the test plots were categorized as "medium" and "difficult" within a three-level categorization system. The categorization followed the forest density criteria presented by Liang et al. [23], who divided boreal forest plots into three categories based on tree density and understory vegetation.

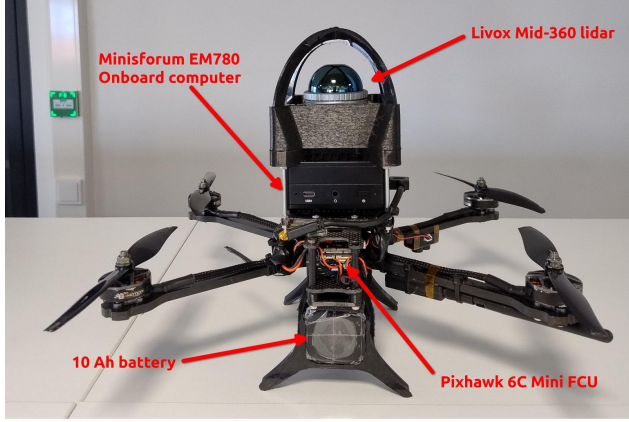


FIGURE 1: The custom-built quadrotor used in the experiments.

Easy forests have a density of less than 700 trees/ha and minimal understory vegetation, medium forests have around 1000 trees/ha with sparse understory vegetation, and difficult forests have approximately 2000 trees/ha and dense understory vegetation. In this study, the medium and difficult plots had approximate tree densities of 1040 trees/ha and 2220 trees/ha, respectively. The main tree species in both plots was Norway spruce (*Picea abies*). The amount of understory vegetation was low, but the spruces had a high number of low-hanging dry branches, increasing the complexity and difficulty of the environment.

The performance of both the original and optimized systems was evaluated through flights in two forest plots at target flight velocities of 1 m/s and 2 m/s. All flights followed a straight-line trajectory from the starting point to a goal point approximately 60 meters ahead. At 1 m/s, 15 flights were conducted per system in each plot totaling 60 flights (30 per system). At target flight velocity of 2 m/s, three flights with the original system were conducted in medium forest, after which the tests were aborted because all flights failed. However, the optimized system completed a full series of 30 flights with a target flight velocity of 2 m/s, including 15 flights in the medium forest plot and 15 flights in the difficult forest plot.

For the flights performed inside the medium forests, the goal point was located in free space except for the first two flights with the original system. The goal area for the flights performed within the difficult forest was situated in a highly cluttered environment. Since there were slight variations between the starting location and orientation of the quadrotor, no large enough obstacle-free area could be located. Thus, the goal point was located inside an obstacle for many flights performed in the difficult forest. Views from the starting locations for both forest plots are shown in Figure 2, and the overhead view of the point clouds obtained from both forest plots is shown in Figure 3.



FIGURE 2: View towards the goal from the starting position of the medium forest plot (a) and the difficult forest plot (b).

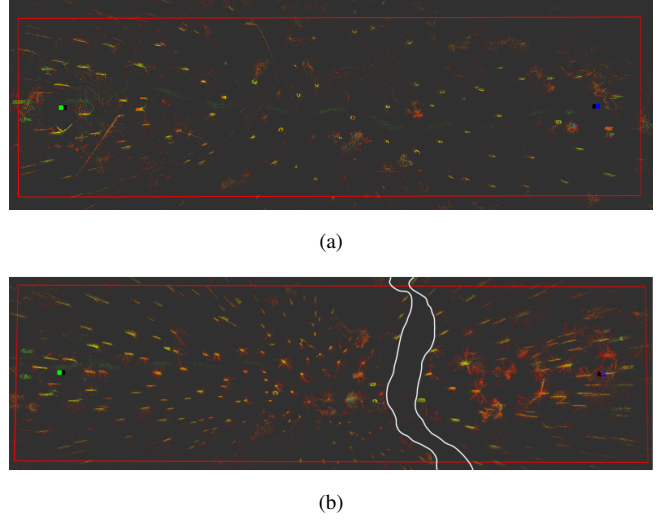


FIGURE 3: Overhead view of the point cloud of the medium forest plot (a) and the difficult forest plot (b). The green cube depicts the starting position (0, 0, 1) and the blue cube depicts the goal position (60, 0, 1), both given in meters. The exact location of the goal position varied between flights since the initial orientation of the quadrotor varied slightly between the flights. The white lines in (b) depict the edges of a trail, after which the denser end of the forest section starts.

Wind conditions were calm during all test flights. The number of leaves on the ground and the number that would be thrust upwards by the quadrotor varied between test flights (Table 1).

The parameters of IPC were set as follows: The obstacle inflation of A^* and the SFC shrinking parameter was set to 0.4 m. The horizon length and time step of MPC were set to 15 and 0.1 s, respectively. The maximum velocity, acceleration, and jerk were set for all directions to 10 m/s, 20 m/s², and 50 m/s³, respectively, except for acceleration downwards, which was set to 9.5 m/s². The MPC problem weight parameters of (1) was set as follows: $R_u = \text{diag}(0, 0, 0)$, $R_p = \text{diag}(2500, 2500, 2500)$, $R_v = \text{diag}(0, 0, 0)$, $R_a =$

TABLE 1: The condition and amount of leaves on the ground, and how often the leaves would be thrust from the ground by the propellers of the quadrotor.

Flight patch	Condition of leaves	Leaves thrust alongside the quadrotor
Original system, medium (1 m/s)	Lot of wet leaves	Occasionally
Original system, medium (2 m/s)	Lot of wet leaves	Occasionally
Original system, difficult (1 m/s)	Lot of frozen leaves	Rarely
Optimized system, medium (1 m/s)	Moist leaves	Occasionally
Optimized system, medium (2 m/s, flights 1-8)	Moist leaves	Occasionally
Optimized system, medium (2 m/s, flights 9-15)	Dry leaves	Often
Optimized system, difficult (1 m/s)	Moist leaves	Occasionally
Optimized system, difficult (2 m/s)	Dry leaves	Often

$\text{diag}(0, 0, 0)$, $\mathbf{R}_{p,N} = \text{diag}(3500, 3500, 3500)$, $\mathbf{R}_{v,N} = \text{diag}(200, 200, 200)$, $\mathbf{R}_{a,N} = \text{diag}(200, 200, 200)$, and $\mathbf{R}_c = \text{diag}(1.0, 1.0, 1.0)$. The forgetting threshold was set to 30 seconds with the original system and to 3 seconds with the optimized system. During preliminary testing with the original system, it was noticed that increasing the forgetting threshold slightly alleviated the up and down movement in place, which was present during the flights with the original system. With the optimized system, the system seemed to perform better when the forgetting threshold was lowered. With the optimized system, the old path following weight parameter w and old path following radius d_{follow} of (2) were set to 150 and 5 m, respectively.

E. PERFORMANCE ASSESSMENT

The performance of both systems was evaluated by measuring the success rate, terminal point, flight time, point-to-point average speed, and average flying speed of the flights. A flight was considered a success if the quadrotor either reached the target goal point or determined, when in close proximity, that the goal point was unreachable. Additionally, the quality of the flights was evaluated visually by identifying undesired behaviors, such as the number of emergency stops, the amount of unnecessary zigzagging, collisions with branches during flights, height estimation discrepancies between flights, and by assessing the general stability of the flights. The average flying speed was calculated by taking the average of the smoothed LTA-OM

approximated velocity over the whole flight. The average flying speed measured how close to the assigned target flight velocity the quadrotor flew. The point-to-point average speed was calculated by dividing the straight line flight distance from the start to the actual terminal point of the flight by the flight time of the flight mission. This can be used to measure how long a flight mission of a certain distance would actually take. By utilizing the point-to-point average speed and the average flying speed of the flights, the time spent solely on flying indirect and crooked paths can be calculated by:

$$t_{\text{extra}} = \frac{d}{v_{\text{p-to-p}}} - \frac{d}{v_{\text{true}}}, \quad (3)$$

where t_{extra} is the time spent flying indirect routes over a certain distance, v_{true} is the average flying speed, $v_{\text{p-to-p}}$ is the point-to-point average speed, and d is the flight distance. If t_{extra} is 0 seconds, then the flight would have taken a completely straight line from start to finish. Therefore, if there are obstacles present between the start and end locations, t_{extra} of exactly 0 seconds cannot be achieved. However, with a perfect system, t_{extra} should be at most only a few seconds over 60 meters even in the difficult forest.

The location accuracy of LTA-OM has been demonstrated to be sufficient for data collection flights inside forests. Zou et al. [14] have conducted experiments with LTA-OM where the location accuracy of LTA-OM was compared against four other lidar-based SLAM algorithms FAST-LIO-SLAM [24], SC-LIO-SAM [25], SC-LeGO-LOAM [26], all proposed by Kim and LiLi-OM proposed by Li et al [27] using the Mulran [28] and NCLT [29] datasets. With LTA-OM, across nine data sequences for both datasets, the average location root-mean-square error (RMSE) was lowest, with an average RMSE of 4.83 m with the Mulran dataset and 1.56 m with the NCLT dataset. Since both datasets were collected inside urban environments and with higher-quality lidar than the Livox Mid-360, these results cannot be transferred directly into forest environments. Thus, in a previous study [30], the performance of LTA-OM was evaluated inside a forest environment with the Livox Mid-360 lidar. The end-point drift of two 150-meter and 420-meter-long manually flown flights was measured. The flights were flown in a forest in Paloheinä, Helsinki. The endpoint drift was 0.19 meters for the 150-meter-long flight and 0.08 meters for the 420-meter-long flight.

III. RESULTS

A. DESCRIPTION OF CAUSES OF FAILURES

The reasons for failure were divided into four categories: a collision with a tree, a collision caused by a cloud of leaves being thrust from the ground around the quadrotor, turning the motors off due to NaNs being generated during the SFC generation process, and a collision resulting from unstable flight.

The most likely reason for failure due to a collision with a tree was that, for some reason, the control command that should steer the quadrotor around a tree led the quadrotor

to fly too close to the tree. This led the quadrotor to think that it is located inside an obstacle. When this happened, to still perform A* replanning, the starting location of the A* search was moved to the closest free voxel in the obstacle map. If the closest free voxel happened to be behind the tree, the quadrotor was directed towards the tree.

A failure caused by a cloud of leaves was due to a similar reason. The leaves that are being thrust around the quadrotor lead the quadrotor to determine that it is located inside an obstacle. Again, the starting location of the reference path was moved to the closest free voxel in the obstacle map. This discrepancy between the current location and the generated reference path sometimes led to a set of very aggressive control inputs or to an MPC solver failure from which it might have been difficult to recover while adhering to the MPC constraints. The extended MPC solver failure might have led to a collision with the surrounding obstacles. However, on many occasions, a cloud of leaves being thrust from the ground did not lead to a failure.

In a failure due to NaNs being generated during the SFC generation process, the corners of the SFC polyhedron were defined as NaNs. If NaNs were not handled, the SFC corner NaN values were forwarded to the MPC problem solver, which in turn generated a set of NaN control commands. These control commands were forwarded to the PX4 FCU, which, in response, turned the motors off.

In a failure due to unstable flying, a collision was caused by a prolonged MPC solver failure. The MPC solver failure happened when the velocity and location of the quadrotor were such that no set of acceptable control actions could have kept the quadrotor inside the SFCs. When this happened, the result from the set of control commands from the last time the MPC solution was solved was used. If the MPC solver failure lasted long enough, the old control commands steered the quadrotor to collide with an obstacle around it. There were different root causes for the prolonged MPC failure, the most prominent being volatile A* path searching. With the original system, every time the path replanning was triggered, A* always tried to find the shortest path towards the goal, which sometimes led to the subsequent reference paths starting in completely different directions. Figure 4 shows an example of how different subsequent planned reference paths have been. In addition to causing prolonged MPC solver failures, especially in highly cluttered areas, it increased the flight completion times significantly as the quadrotor flew around the same position for long durations.

Table 2 provides an overview of the results of the flights, and a more detailed overview of the individual flights is presented in the Appendix. A summary of the number of failures by cause for both system versions across all flight velocities and forest difficulty levels is shown in Table 3.

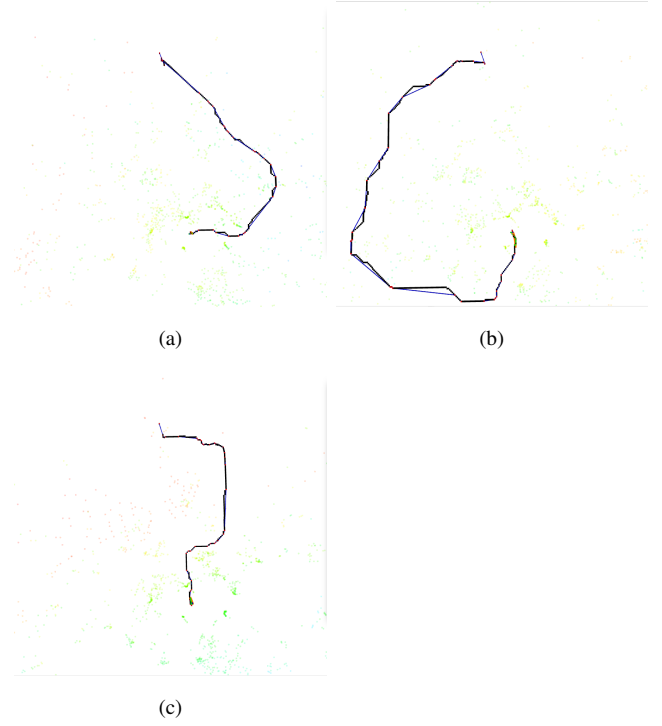


FIGURE 4: An example of volatile A* reference path planning from flight 10 of the flights done with the original system in the difficult forest. The black line depicts the optimal planned A* path, and the blue line depicts the output flight path. The time interval between the first picture (a) and the last picture (c) was approximately 1.2 seconds.

B. FLIGHT TESTS WITH THE ORIGINAL SYSTEM

1) FLIGHTS IN THE MEDIUM FOREST

A total of 10/15 flights were successful with the original system in the medium forest with a target flight velocity of 1 m/s (Tables 2 and 4). Of the five failed flights, two failures were due to a cloud of leaves being thrust from the ground around the quadrotor, one was due to a collision with a tree, one was due to NaNs being generated during the SFC generation procedure, and one was due to unstable flying. In addition to the failed flights, there were six instances of a cloud of leaves being thrust from the ground, after which the quadrotor managed to continue flying successfully. During five of the ten successful flights, there were collisions with small branches or with the ground, after which the quadrotor successfully managed to continue flying. During the third and 14th flights, there were long periods of flying around the same position due to volatile A* path searching. In general, in the medium forest, flying was stable with occasional aggressive maneuvers when dodging leaves or near obstacles. This can be seen in Figure 5a as a low number of zigzags and aggressive turns in flight paths.

There were significant differences between the height estimation of LTA-OM. Although no location ground truth

TABLE 2: Overview of all flight experiments. Point-to-point average speed, average flying speed, and t_{extra} were measured for only successful flights. An "x" indicates that no data was collected

Algorithm, forest difficulty and target velocity	Success rate	grand mean point-to-point speed	grand mean flying speed	t_{extra} from the average speeds
Original system				
Medium forest, 1 m/s	10/15	0.68 m/s	0.76 m/s	9.3 s
Medium forest, 2 m/s	0/3	x	x	x
Difficult forest, 1 m/s	6/15	0.44 m/s	0.70 m/s	50.6 s
Optimized system				
Medium forest, 1 m/s	12/15	0.76 m/s	0.80 m/s	3.1 s
Medium forest, 2 m/s	12/15	1.35 m/s	1.48 m/s	3.8 s
Difficult forest, 1 m/s	15/15	0.66 m/s	0.74 m/s	9.5 s
Difficult forest, 2 m/s	5/15	1.06 m/s	1.32 m/s	11.5 s

TABLE 3: Overview of the failure reasons for all flight experiments. *With the original system inside the medium forest, with a target flight velocity of 2 m/s, only three flights were performed.

Algorithm, forest difficulty and target velocity	Hit a tree	Cloud of leaves	NaN SFC	Unstable flying	Total
Original system					
Medium forest, 1 m/s	1	2	1	1	5
Medium forest, 2 m/s*	0	0	0	3	3*
Difficult forest, 1 m/s	3	0	4	2	9
Optimized system					
Medium forest, 1 m/s	0	3	0	0	3
Medium forest, 2 m/s	0	2	0	1	3
Difficult forest, 1 m/s	0	0	0	0	0
Difficult forest, 2 m/s	2	5	0	3	10

data was collected during the flights, based on visual observations, significant height differences were present. Figure 6 shows the terminal location of flights eight and nine. The LTA-OM estimated height of the eighth flight was 1.00 meters, and 0.98 meters for flight nine. However, from Figure 6 it can be seen that the heights were actually approximately 30 cm apart.

The average flying speed of the quadrotor was lower than the target flight velocity of 1 m/s, ranging between 0.60 m/s and 0.81 m/s, with the grand mean flying speed being 0.76 m/s (Tables 2 and 4). Moreover, the point-to-point average speed was even lower, ranging from 0.43 m/s to 0.77 m/s, with the grand mean point-to-point speed being 0.68 m/s. On average, the 60-meter flight missions took 89.2 seconds to complete. The longest flight mission lasted 133.8 seconds, while the shortest lasted 75.2 seconds. Most flights were completed in approximately 80 seconds, with three flights taking significantly longer. The first two flights took longer because the goal point was located inside a bush, requiring the system to survey the path before determining that the goal

point was unreachable. During the 14th flight, due to a cloud of leaves, the quadrotor got stuck inside a tight cluster of trees, which caused the system to stop in place and determine that the goal was unreachable. The goal command was given multiple times before the system managed to clear the cluster of trees. Due to these reasons, t_{extra} was large for flights 1, 2, and 14, being 22.7, 17.0, and 39.4 seconds, respectively. For other successful flights, t_{extra} remained smaller, ranging between 2.0 and 12.6 seconds.

All flights failed before 20 meters with a target flight velocity of 2 m/s when the volatile A* replanning led to a prolonged MPC failure (Tables 2 and 5). After three flights, it was deemed highly unlikely that the original system could perform any successful flights. To avoid hardware damage during collisions, no more flights were performed with the original system with a target flight velocity of 2 m/s.

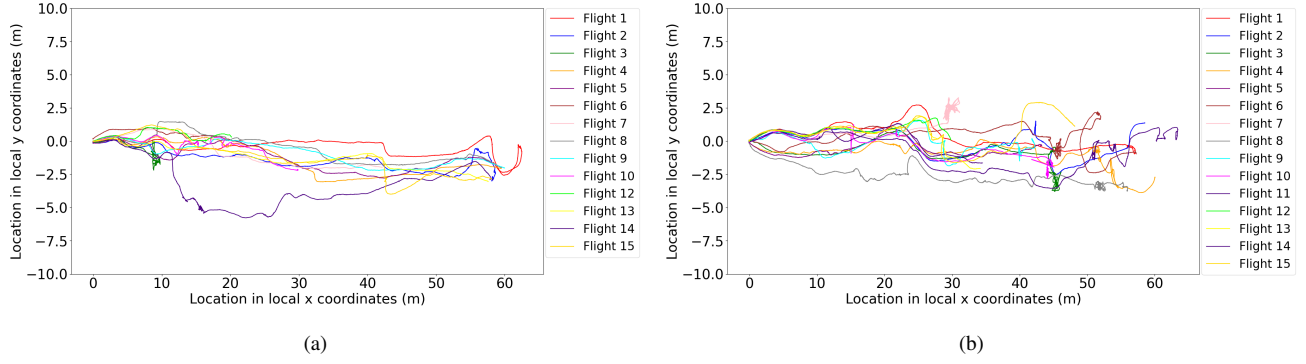


FIGURE 5: The LTA-OM approximated flight paths of all flights flown with a target flight velocity of 1 m/s in the medium forest (a) and in the difficult forest (b) with the original system. The flight paths are given in the local coordinates of individual flights, which means that the same location on the graph does not necessarily correspond to the same location in the test area. For the flights done in the medium forest (a), the rosbag recording of flight 11 was lost and is thus omitted from the graph. For the flights done in the difficult forest (b), the rosbag recording of flight 7 was cut short, but the terminal point of that flight is very close to the one depicted in the graph.

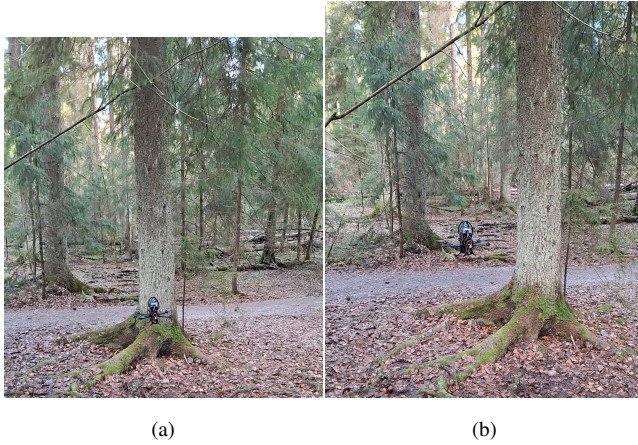


FIGURE 6: The terminal locations of flights eight (a) and nine (b) performed in the medium forest with the original system. The height difference of approximately 30 cm is clearly visible between the two flights. The difference in the xy-plane is due to a slightly different orientation of the starting location.

2) FLIGHTS IN THE DIFFICULT FOREST

With the original system, six of the fifteen flights were successful in the difficult forest with a target flight velocity of 1 m/s (Tables 2 and 6). Of the nine failed flights, three were due to a collision with a tree, four were due to NaNs being generated during the SFC generation process, and two were due to unstable flying. None of the failures was due to a cloud of leaves being thrust around the quadrotor. In fact, there were almost no instances of a cloud of leaves interrupting normal flying during these test flights. On three of the six successful flights, there were collisions with small

branches. Both slight collisions and collisions leading to a failed flight were especially numerous, in the denser end of the site, after the trail depicted in Figure 3b. During every flight, there were extended periods of volatile A* replanning, which led to long periods of flying around the same point. The most prominent example of this was during the seventh flight, where the quadrotor got stuck flying around the same area inside a dense group of trees for approximately six minutes. During these periods, the quadrotor was most likely to have collisions with small branches. In general, flying was unstable with a lot of aggressive maneuvers and repetitive flying in place, which can be seen in Figure 5b as a high number of zigzags and aggressive turns in flight paths.

The average flying speed was significantly lower than the target flight velocity of 1 m/s, ranging between 0.64 m/s and 0.76 m/s for successful flights, with a grand mean flying speed of 0.70 m/s (Tables 2 and 6). Moreover, the point-to-point average speed was significantly lower across all flights. The lowest point-to-point average speed was 0.31 m/s, and the highest was 0.59 m/s, with a grand mean of only 0.44 m/s. Thus, on average, the 60-meter flight missions took 144.3 seconds to complete. The variation in flight mission completion times was large, with the shortest taking 94.8 seconds and the longest taking 194.7 seconds. Most successful flights, namely 4 out of 6, were over 140 seconds long. The main reason for very long flight mission completion times was long and frequent in-place flying periods. These periods can be seen in Figure 5b as clusters of zigzags in the flight paths, for example, at the location around 45 m. The long times spent flying unnecessarily long routes can be verified by examining t_{extra} of the flights. On 3 out of 6 successful flights, over 85 seconds were spent flying longer routes over a distance of 60 meters. There was only one flight where t_{extra} remained small, at 7.9 seconds.



FIGURE 7: The fallen tree, to which flights 11 and 15 of the optimized system, in a medium forest with a target flight velocity of 1 m/s, collided with.

C. FLIGHT TESTS WITH THE OPTIMIZED SYSTEM

1) FLIGHTS IN THE MEDIUM FOREST

A total of 12 out of 15 flights were successful in the medium forest with a target flight velocity of 1 m/s (Tables 2 and 7). In all failure instances, the quadrotor was flying close to the ground when leaves were thrust upward. The system tried to dodge the leaves by going under them, which led to a collision with the ground. Nevertheless, on most occasions, a cloud of leaves did not result in a failure. In 10 of the 12 successful flights, the system had to dodge leaves at least once. During the 11th and 15th flights, the quadrotor slightly hit a fallen tree with its landing gear (Figure 7). After the collision during the 11th flight, the quadrotor did not manage to find a route towards the goal, and the goal command had to be reissued. The quadrotor was flying in place for approximately 12 seconds. In general, the flights were smooth, with few aggressive maneuvers, except when avoiding leaves or navigating near obstacles. This can be seen in Figure 8a as almost no zigzags or aggressive turns in the flight paths.

The variation between the average flying speed and the average point-to-point speed was small (Tables 2 and 7). The average flying speed was lower than the target flight velocity of 1 m/s, ranging from 0.70 m/s to 0.84 m/s, with the grand mean flying speed of 0.80 m/s. The point-to-point average speed ranged between 0.65 and 0.79 with a grand mean of 0.76 m/s. Thus, on average, the 60-meter flight missions lasted 78.7 seconds. The longest flight times were 93.1 and 81.7 seconds, while the shortest was 75.6 seconds.

Due to linear and non-zigzag routes taken, t_{extra} remained small; t_{extra} varied between 0.7 and 6.6 seconds.

The flights in the medium difficulty forest at a target flight velocity of 2 m/s were flown during three separate days (Table 8). The first eight flights were conducted on the first day, the ninth flight on the second, and the last six flights on the third day. During the first eight flights, there were a lot of moist leaves on the ground, which were sporadically thrust from the ground. During the last seven flights, there were a lot of dry leaves on the ground, which would often be thrust from the ground.

With the optimized system, 12 out of 15 flights at the target velocity of 2 m/s were successful (Tables 2 and 8). Two of the failed flights were due to a cloud of leaves, and one was due to unstable flying caused by a prolonged MPC solver failure. In the seventh flight, the quadrotor was flying close to the ground when a cloud of leaves was thrust from the ground, which caused the quadrotor to try to dodge the leaves by flying downwards. This resulted in a collision with the ground. In the ninth flight, a cloud of leaves led to a prolonged MPC failure, which caused the quadrotor to fly towards the sky. The flight was terminated manually by triggering the kill switch of the motors at high altitude. The resulting crash with the ground was severe enough to damage the quadrotor, for which reason the rest of the test flights for the day were canceled. In the tenth flight, the quadrotor did not notice a small spruce behind another tree, which resulted in a prolonged MPC failure and a collision with the ground. During the first eight flights, the system had to dodge some leaves during three flights. During the last seven flights, the system had to dodge some leaves multiple times per flight. In general, flying with a target velocity of 2 m/s was more unstable than with a target flight velocity of 1 m/s. During four of the successful flights, there were moments when the system dodged an obstacle or a cloud of leaves very aggressively. During two of these flights, the quadrotor collided with the ground but managed to continue flying. Additionally, during the 13th flight, a cloud of leaves caused the quadrotor to fly up towards the branches of the tree, which caused the quadrotor to flip over 90 degrees from the horizontal plane. The quadrotor managed to stabilize itself and continue flying normally after three seconds of staying put after detecting NaNs during the SFC generation. These moments can be seen in Figure 8b as aggressive turns in flight paths.

The variation of the average flight speed was small (Tables 2 and 8). The average flying speed was lower than the target flight velocity of 2 m/s, ranging from 1.23 m/s to 1.58 m/s, with a grand mean flying speed of 1.48 m/s. The second lowest average flying speed was 1.42 m/s. The point-to-point average speed ranged between 1.14 m/s and 1.51 m/s, with a grand mean of 1.35 m/s. Although the absolute difference between the average flight speed and the point-to-point average speed was larger, the larger absolute speed of the quadrotor meant that t_{extra} remained small across

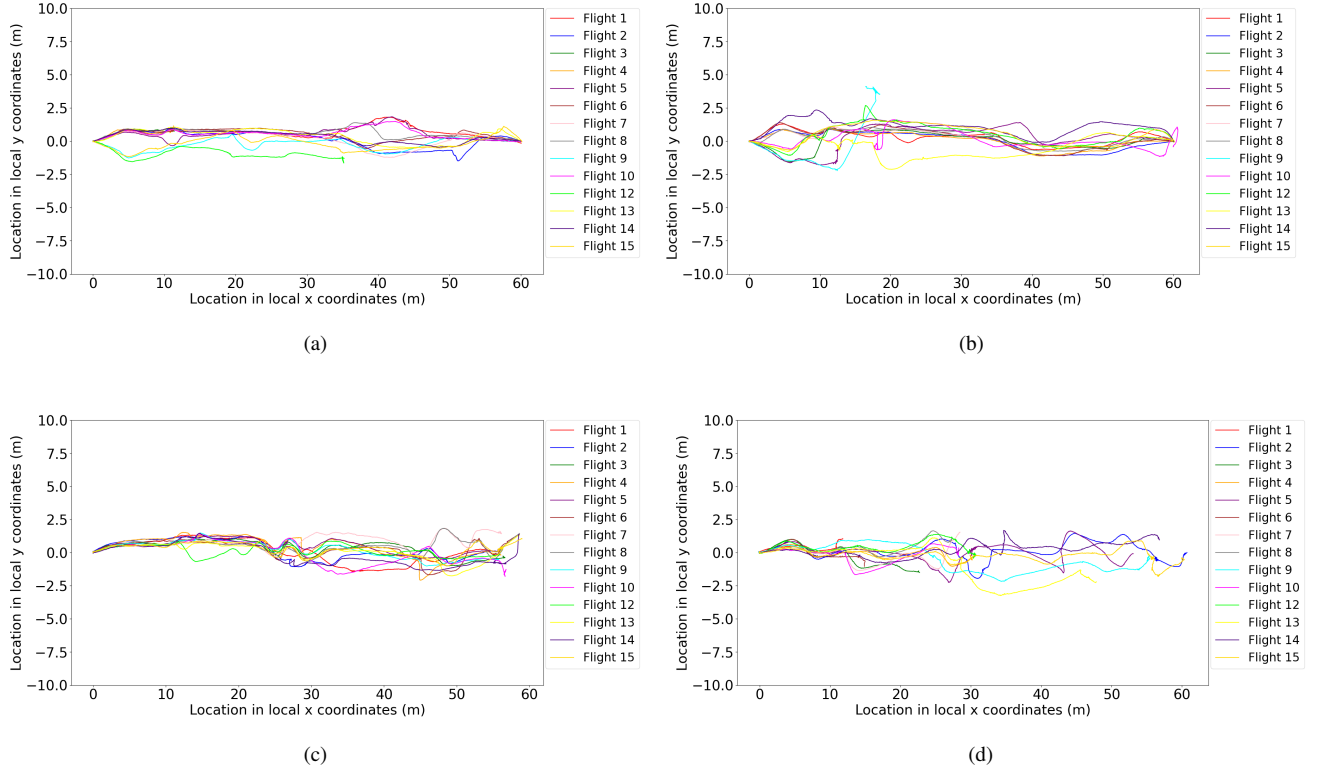


FIGURE 8: The LTA-OM approximated flight paths of all flights flown with the optimized system. (a) and (b) show the flight paths flown in the medium forest, and (c) and (d) in the difficult forest. The flight paths are given in the local coordinates of individual flights, which means that the same location on the graph does not necessarily correspond to the same location in the test area. Flights (a) and (c) were flown with a target flight velocity of 1 m/s, while (b) and (d) were flown at 2 m/s.

all flights. t_{extra} ranged from 1.2 to 9.5 seconds. The flight mission completion times ranged from 39.6 seconds to 51.7 seconds with an average of 41.3 seconds. With the optimized system, the system performed emergency stops when it failed to find a path towards the goal within 0.1 seconds. These were most numerous right at the beginning of the flights. On most occasions, the emergency stop lasted for only a fraction of a second, but on five flights, the emergency stop procedure lasted longer. During those flights, the estimated duration of a single set of emergency stops varied between 0.5 and 3.0 seconds. During the 15th flight, there was an emergency stop period, which ended in the system determining that no path towards the goal was found. Thus, after 11 seconds, the goal command was regiven.

With both flight speeds, there were no visually visible height estimation differences of LTA-OM. Based on visual observations of the quadrotor hovering in the goal point, the quadrotor seemed to be hovering at the same height across all completed flights.

2) FLIGHTS IN THE DIFFICULT FOREST

All 15 flights conducted in the difficult forest at a target velocity of 1 m/s were successful (Tables 2 and 9). In general, flying was relatively stable with only a few aggressive dodges, excluding the emergency stops done after the A* path planning took over 0.1 seconds to complete. The relatively stable flying can be seen in Figure 8c where there were only a few aggressive turn in the flight paths. In four of the flights, there were minor collisions with branches or with a tree trunk. In seven of the flights, the quadrotor had to avoid leaves that were raised from the ground. However, the cloud of leaves was smaller than, for example, during flights conducted in medium difficulty forests with the optimized system.

Since the goal point was located in a very dense area, the quadrotor had problems finding a route to the goal point. Thus, during every flight, at least once near the goal point, the A* path search took longer than 0.1 seconds to complete, which triggered the emergency stop procedure. On most flights, the emergency stop procedure was triggered 1-4 times. However, during flights the 6th and 14th flight, an emergency stop procedure was triggered ten and nine times,

respectively. Additionally, ten flights ended in an emergency stop when the quadrotor deemed that no path to the goal was found. In the remaining five flights, the flight ended near the goal point, which was moved by the path planner module since the goal point was deemed to be located inside an obstacle.

The average flight speed was lower than the target velocity of 1 m/s, ranging from 0.62 m/s to 0.79 m/s, with a grand mean of 0.74 m/s (Tables 2 and 9). The point-to-point average speed varied between 0.51 m/s and 0.73 m/s, with a grand mean of 0.67 m/s. The flight times ranged from 76.6 to 115.9 seconds with an average of 86.5 seconds. t_{extra} remained small across most flights, ranging from 4.0 to 22.6 seconds. In the difficult forest, the emergency stops, due to the A* module taking too long to find a path towards goal, took a longer time than in the medium forest. Most of the emergency stop period lasted for a few tenths of a second to a couple of seconds. On most flights, the total time spent in the emergency stop periods ranged from 0 to 6 seconds. However, on two flights (6 and 14), these periods lasted 26 and 22 seconds, respectively.

In the difficult forest, 5 out of 15 flights were successful with a target flight velocity of 2 m/s (Tables 2 and 10). Out of the ten unsuccessful flights, five were due to a cloud of leaves, three due to unstable flying, and two due to a collision with a tree. On one out of the five successful flights, there were two slight collisions with branches. As was the case with the flights done with a target flight velocity of 1 m/s, there were numerous emergency stops conducted, especially after the trail due to A* path searching taking too much time. There were 1-8 emergency stops performed during every successful flight, with some being performed right at the start, as was done in the medium forest with a target flight velocity of 2 m/s. Three of the successful flights ended by the system determining that no path to the goal could be found, and two of the successful flights terminated near the goal position, which was moved by the path planner module. In general, flying was more unstable than with a target flight velocity of 1 m/s or in medium forest. This can be seen in Figure 8d as a higher number of aggressive turns in the flight paths.

The average flying speed was significantly lower than the target flight velocity of 2 m/s, ranging between 1.06 m/s and 1.56 m/s, with a grand mean of 1.32 m/s (Tables 2 and 10). The point-to-point average speed varied between 0.79 m/s and 1.35 m/s, with a grand mean of 1.06 m/s. The flight times ranged between 42.0 and 76.1 seconds with an average of 56.8 seconds. t_{extra} ranged from 6.0 to 19.3 seconds. Out of the five successful flights, in three, the total time spent in the emergency stop periods ranged from 1 to 3 seconds. However, during the rest of the successful flights, namely flights 2 and 15, 10 and 19 seconds were spent in the emergency stop periods, respectively.

D. ANALYSIS OF THE RESULTS AND THE COMPARISONS BETWEEN THE ORIGINAL AND OPTIMIZED SYSTEM

The performance of the original system was poor, especially in the difficult forest. With a success rate of only 40% and an average of nearly a full minute spent flying indirect and zigzag routes, the original system is unsuitable for flights inside forests. Although the performance of the original system was much better in the medium forest, the reliability should be improved. Moreover, the original system failed to complete any flights at the target velocity of 2 m/s. Thus, reducing the completion times of the flight mission by increasing the target flight velocity with the original system would be inadvisable. Given the poor performance of the original system, particularly in the difficult forest, the optimized system aimed to improve reliability, reduce mission completion times by minimizing t_{extra} , and increase the average flight speed without compromising reliability. Additionally, there was a problem with the height estimation in the medium forest with the original system.

The reliability of the optimized system was substantially better than that of the original system. With a target flight velocity of 1 m/s, the success rate improved from 10 out of 15 to 12 out of 15 successful flights in the medium forest and from 6 out of 15 to 15 out of 15 successful flights in the difficult forest. The main reason for the improved reliability was the less volatile A* path planning of the improved reference path searching module. It made flying more stable in general and reduced the number of aggressive maneuvers made, especially in cluttered areas. The more stable flying of the optimized system can be seen in the flight paths shown in Figures 5 and 8. There is no zigzagging in the flight paths of the optimized system, and fewer aggressive turns across all flight paths than with the original system. The other improvement was the handling of NaNs during the SFC generation process. Although the error handling was simple in its design and sometimes led to long periods of flying stationary in place, it eliminated the failures related to NaNs completely. The cloud of leaves posed some problems even with the optimized system. In fact, all failures with a target flight velocity of 1 m/s were caused by a cloud of leaves. However, the optimized system seemed to perform better than the original system around a cloud of leaves. Although the failure numbers remained similar across both systems, there were more lightweight leaves on the ground during the experiment conducted with the optimized system, which led to more leaves being lifted from the ground by the propellers. Overall, effectively handling clouds of leaves rising from the ground remains a major challenge for the optimized system. Lastly, the optimized system resolved the height estimation issue present in the original system. Due to the use of gravity direction measurements, the end-point height of flights was maintained consistently.

The more stable flight and improved reliability of the optimized system were particularly evident with the flights

done at the target flight velocity of 2 m/s. With the original system, none of the flights were completed, even in the medium forest. In contrast, the optimized system successfully completed 12 out of 15 flights in the medium forest.

There was no significant reduction in reliability with the optimized system with a target flight velocity of 1 m/s when the forest was more difficult. In fact, the success rate rose from 12 out of 15 to 15 out of 15 from the medium forest to the difficult forest. Thus, based on the results of the experiment, the reliability of the system is not strictly affected by the density of the forest with low target flight velocities.

The reliability of the optimized system decreased when the target flight velocity increased from 1 m/s to 2 m/s in both forest densities, especially in the difficult forest. Although 12 out of 15 flights in the medium forest were successful at both target flight velocities, the decrease in reliability was primarily due to generally less stable flight, which caused more collisions with branches that did not result in mission failures. However, the decrease in reliability was minor. In the difficult forest, the performance degradation was large. The success rate dropped from 15 out of 15 to 5 out of 15. Moreover, overall flight stability decreased substantially, and failures not due to leaves increased significantly.

The completion times of the flight mission decreased with the optimized system compared to the original system. The average flight mission completion time was reduced from 89.2 seconds to 78.7 seconds in the medium forest. With a target flight velocity of 2 m/s, the average flight completion time was reduced even further to 41.3 seconds. In the difficult forest, the flight mission completion times reduced from 144.3 seconds to 86.5 seconds with a target flight velocity of 1 m/s and to 56.8 seconds with a target flight velocity of 2 m/s. The primary reason for the decrease in flight times was the elimination of in-place zigzag maneuvers in the original system. In the medium forest, t_{extra} reduced from 9.3 seconds to 3.1 and 3.8 seconds with the target flight velocities of 1 m/s and 2 m/s, respectively. In the difficult forest, the difference was larger, reducing from 50.6 seconds to 9.5 and 11.5 seconds with the target flight velocities of 1 m/s and 2 m/s, respectively. Moreover, the optimized system achieved a slight increase in average flight speed from 0.76 m/s to 0.80 m/s in the medium forest and from 0.70 m/s to 0.74 m/s in the difficult forest.

With the optimized system, the flight mission completion times increased only slightly when moving from the medium to the difficult forest. The main reason for the increase in flight times, in addition to there being more obstacles that take time to dodge, was the emergency stop periods due to prolonged A* path searching near the cluttered goal area in the difficult forest. Although on most flights, the combined duration spent in emergency stop periods was small, there were flights where it took over 20 seconds.

IV. DISCUSSION

A. ANALYSIS OF SYSTEM PERFORMANCE AND WAYS TO IMPROVE THE SYSTEM

The optimized system showed good performance, especially with low target flight velocities. The success rates of 12 out of 15 and 15 out of 15 with the target flight velocity of 1 m/s make the optimized system well-suited for under-canopy forest flights. Especially if failures due to clouds of leaves are excluded, the optimized system achieves a 100% success rate. However, since the reliability of the system is mainly hindered by leaves, developing a solution for ignoring leaves and other lightweight loose foliage would make the system more reliable and usable all year round.

The experiments indicate that increasing the target flight velocity from 1 m/s to 2 m/s is not advisable in difficult forests, due to a substantial decrease in system reliability. In medium and easier forests, flying with a target flight velocity of 2 m/s could be feasible. System reliability remained similar at both target flight speeds, while mission completion times decreased at the higher flight speed. However, the less stable flying combined with the higher speed could degrade the quality of the final application, such as captured remote sensing datasets. This might be especially impactful if the data collection were done with cameras alongside lidar.

Since forests are not homogeneous in their density and difficulty to fly through, and since the optimized system showed differing performance when the target flight velocity was increased in a difficult forest, having the ability to adapt the target flight velocity based on density and difficulty of the upcoming forest patch would be beneficial. This could be done based on the density of the obstacle map and the amount of estimated free space around the planned path. If the obstacle density is low and if there is a lot of free space around the planned path, the target flight velocity could be increased and decreased if a patch of denser forest is detected. Adaptive target flight velocity could allow the system to fly faster in sparser areas and slower and more safely in denser areas.

Another way to improve system reliability is to define a safety margin around obstacles, within which paths are not planned unless no alternative route to the goal exists. Since A* seeks an optimal path towards the goal, the resulting path passes obstacles as close as possible to minimize path length. This increases the risk of a collision with the obstacle. With an additional safety radius, the system could dodge obstacles at a greater distance when possible, but still go through tight gaps when necessary.

B. COMPARISON TO OTHER SYSTEMS

Comprehensive comparisons with other under-canopy flying quadrotors are challenging due to incomplete performance metrics reported in earlier studies. Ren et al. [3] have flown multiple high velocity flights with a 100% success rate in sparse-looking forest environments where it could utilize paths going through the forest. It has also followed human

targets in a cluttered forest-like environment, which has no low-hanging branches. Moreover, they have performed an experiment that shows that the autonomous solution can successfully dodge thin objects. It could dodge all thin wires with the thinnest being 2.5 mm in diameter. Zhou et al. [5] have performed at least one flight without a reported success rate in a dense-looking forest with a low amount of low-hanging branches as a swarm. Based on the experiments conducted by the original authors, comparing the reliability of the optimized system to other algorithms is very difficult. Although [3] showed very promising results, the performance and the reliability of the system inside dense forests remain unknown.

Karjalainen et al. [10] have performed more thorough experiments with a system based on the algorithm proposed by Zhou et al. [5]. Seven flights were performed in a medium forest, with a tree density of 650 trees/ha with some low-hanging branches, and eight flights were performed in a difficult forest, with a tree density of 2000 trees/ha with some low-hanging branches. The flight distances varied between 34 and 42 meters. The success rate of flights in the medium forest was 100% and 87.5% in the difficult forest. The flight speed was not reported, although in the previous experiments conducted by Karjalainen et al., the target flight speed was 1 m/s in similar difficulty forests [9].

Overall, the optimized system performed slightly better than the system of Karjalainen et al. Although the reliability of the optimized system in the medium forest was lower (80%), the reliability in the difficult forests was higher (100%). Moreover, the test forests flown in by Karjalainen et al. were slightly easier than the test forest used in this paper. Additionally, the flight distances flown by Karjalainen et al. were considerably shorter than those in this paper.

C. STANDARDIZED EXPERIMENTAL SETUP

To make it possible to compare and evaluate the performance and the applicability of different autonomous flying solutions, the testing schemes and reporting should be improved within the scientific community. Currently, the experimental setup and reporting lack important details. First, the forest test areas are not described in sufficient detail. Often, the test forests are only described as "dense" with minimal other information. In the literature, based on the available information, such as on-site pictures, supplementary videos, and overhead point clouds of the test area, "dense" forests seem to vary a lot in difficulty. Often, the forests seem to be on the easy side of the forest complexity criteria used in this paper. Additionally, sometimes the flight paths are aligned so that there are very few obstacles between the start and goal points, or there are paths that the drone can use to easily traverse the forest. Second, on many occasions, the success rate of real-world flights is not reported. If it is only stated that the proposed system managed to fly through a forest plot without performing and reporting on multiple flights, the reliability of the system cannot be evaluated.

Thus, a more standardized testing setup is proposed where the difficulty of the forest, the success rate, and the actual flight speed of the flights should be reported. First, the tree density and difficulty of the forest should be reported more precisely. The difficulty of the forest is comprised of two major factors: the density and amount of trees, and the amount of branches and other foliage. The amount of low-hanging branches and other foliage is especially important for the difficulty of the forest when flying close to the ground. Both of these factors should be reported. Additionally, a visual representation of the test forest should be provided by including, for example, under-canopy pictures of the test forest alongside a point cloud collected from the test area. The presence of anomalies, such as leaves on the ground, should also be reported. Second, the success rate of flights should be reported by performing multiple flights through a route that well represents the forest in question. The flight path should be aimed so that there are no obstacles on the direct path between the start and the goal. In addition, there should not be any parallel paths that the autonomous flying system could utilize to easily dodge the trees. Ideally, multiple flights should be performed in multiple forest locations with varying levels of difficulty. Measuring the success rate of multiple flights is the only way to determine the reliability of the system. The length of the flights should be reported. Lastly, in addition to the target flight speed, the actual flight speed should be reported alongside the flight mission completion times.

In addition to the performance metrics related to the autonomous flying performance of the system, the localization accuracy of the proposed system should be demonstrated. Ideally, this should be done by collecting ground truth data of the autonomously flown path and comparing the location estimation of the localization system to the ground truth by calculating, for example, the RMSE between the estimated path and the ground truth. However, obtaining an accurate reference trajectory can be challenging. Real-time kinematic positioning (RTK) GNSS is an attractive option, but its precision and reliability degrade in forested environments. Other methods for obtaining an accurate ground truth have been used. For example, Karjalainen et al. [10] estimated the reference trajectory using a structure-from-motion technique with ground control points measured by a robotic tachymeter. Since this process can be laborious, we propose that for rapid testing, it is sufficient to demonstrate localization accuracy, for example, by manually flying the quadrotor in the forest and measuring the end-point drift of the position estimate, as done by Karhunen [30]. For a comprehensive analysis, however, the more rigorous full trajectory estimation should still be performed. Using solely the widely used benchmarking datasets, such as Mulran [28], EuRoC MAV [31], or KITTI [32], cannot be considered satisfactory since they lack flight data inside forests or are not collected with UAVs.

If the experimental setup presented above were applied to novel autonomous under-canopy algorithms and solutions,

it would facilitate comparisons of different autonomous flying systems based on literature alone. Ideally, all systems should be tested at the same location and time to enable direct performance comparisons. Since this is rarely feasible, adopting the experimental setup proposed in this paper would substantially improve the comparability of different frameworks.

Simulation can be considered a fundamental approach for system testing, especially as a form of preliminary testing. However, for under-canopy quadrotors, relying solely on simulation experiments, at least with current state-of-the-art simulators, does not accurately reflect the system's real-world performance. The complexity of the real-world forest, combined with the chaotic nature of the real-world, often means that the simulation is not representative of the real-world autonomous flights. Thus, a set of well-reported and documented real-world experiments is a necessity for proving the performance and reliability of the proposed systems.

Alongside the improved comparability, this paper demonstrates an additional benefit of extensive experimentation. Based on the experiments conducted with the original system, the performance of the system was improved significantly with a set of modifications. The optimized system was capable of flying with a 100% success rate in the selected medium and dense forest environments, excluding a few failures caused by loose flying leaves. Indeed, the study highlighted a new challenge posed by loose leaves for lidar-based autonomous flying quadrotors, which will require further development in the future.

V. CONCLUSION

In this paper, a light-weight lidar-based autonomous flying quadrotor system was implemented, and its performance was evaluated by performing a set of extensive field experiments. A miniaturized forest drone equipped with a lightweight lidar weighing only 1.2 kg (excluding batteries) was developed, and openly available code was implemented for autonomous navigation. Based on the experimental results, the original system was further enhanced. The performance of the optimized system was evaluated and compared against the original system based on the thorough experiments conducted in the same location. The systems were evaluated by flying 93 60-meter-long flights inside two different difficulty forests with two different target flight velocities.

Based on the results of the experiments, the optimized system showed significantly better performance than the original system. The reliability of the optimized system, measured by flight success rates, was significantly better, especially in the difficult forest with a target flight velocity of 1 m/s and in all forests with a target flight velocity of 2 m/s. There was a significant reduction in flight completion times with the optimized system due mainly to a reduced amount of in-place zigzagging.

The optimized system could be further developed by developing a way to ignore leaves and other lightweight foliage that might be thrust onto the path of the quadrotor by its propellers. With the current system, the leaves are detected as obstacles that might lead to a collision with the surrounding obstacles. Adaptive velocity tracking could reduce the flight times inside sparse forest regions by increasing the target flight speed while increasing reliability by decreasing the target flight speed in denser areas. The reliability of the system could also be improved by creating an extra safety area around obstacles, which would force the quadrotor further away from obstacles, given that there is enough free space around the planned path. If the space between obstacles is small, a path can be planned through the extra safety area.

The performance of the optimized system was compared against other autonomous flying systems as reported in the literature. However, due to non-extensive field experiments and reporting on most systems, accurate comparisons were difficult to make.

Therefore, a standardized testing scheme was proposed for assessing the performance of autonomously navigating drone algorithms in forest environments. In this scheme, multiple flights should be conducted, preferably multiple flights in multiple different forest difficulties with multiple target flight velocities, and the success rate of all flights should be reported. The difficulty of the forests should be reported based on their tree density, amount of low-hanging branches, and understory vegetation. Both the intended flight distance and the actual flight speed should be reported. The location accuracy of the system should be demonstrated by flying the quadrotor inside a forest environment. By using standardized testing schemes, the performance of different autonomous flying systems could be compared based on the literature alone. Such comparisons could greatly support the further implementation of robotic algorithms for under-canopy drones, guide improvements to these systems, and potentially lead to further breakthroughs in forest robotics and autonomous UAV navigation.

In the future, our aim is to deploy the autonomously navigating under-canopy drone as a less labor-intensive way of collecting data inside forests. The quadrotor system could be equipped with, for example, cameras that can be used for data image collection. Interesting applications for the system include stem measurements of trees and bark beetle infestation detection, to name a few potential applications.

REFERENCES

- [1] F. M. Schubert, B. H. Fleury, P. Robertson, R. Prieto-Cerdeira, A. Steingass, and A. Lehner, "Modeling of multipath propagation components caused by trees and forests," in *Proceedings of the Fourth European Conference on Antennas and Propagation*, 2010, pp. 1–5.
- [2] W. Liu, Y. Ren, and F. Zhang, "Integrated planning and control for quadrotor navigation in presence of suddenly appearing objects and disturbances," *IEEE Robotics and Automation Letters*, vol. 9, no. 1, pp. 899–906, 2024.
- [3] Y. Ren, F. Zhu, G. Lu, Y. Cai, L. Yin, F. Kong, J. Lin, N. Chen, and F. Zhang, "Safety-assured high-speed navigation for mavs," *Science*

- Robotics*, vol. 10, no. 98, p. eado6187, 2025.
- [4] A. Sharma and E. Liang, "Autonomous quadrotor navigation using lidar slam and adaptive tree-based path planning in simulation," in *2024 Sixth International Conference on Intelligent Computing in Data Sciences (ICDS)*, 2024, pp. 1–10.
 - [5] X. Zhou, X. Wen, Z. Wang, Y. Gao, H. Li, Q. Wang, T. Yang, H. Lu, Y. Cao, C. Xu, and F. Gao, "Swarm of micro flying robots in the wild," *Science Robotics*, vol. 7, no. 66, p. eabm5954, 2022.
 - [6] L. Campos-Macías, R. Aldana-López, R. de la Guardia, J. I. Parra-Vilchis, and D. Gómez-Gutiérrez, "Autonomous navigation of mavs in unknown cluttered environments," *Journal of Field Robotics*, vol. 38, no. 2, pp. 307–326, 2021.
 - [7] Z. Xu and K. Shimada, "Quadcopter trajectory time minimization and robust collision avoidance via optimal time allocation," in *2024 IEEE International Conference on Robotics and Automation (ICRA)*, 2024, pp. 16 531–16 537.
 - [8] J. Tordesillas and J. P. How, "FASTER: Fast and safe trajectory planner for navigation in unknown environments," *IEEE Transactions on Robotics*, 2021.
 - [9] V. Karjalainen, T. Hakala, A. George, N. Koivumäki, J. Suomalainen, and E. Honkavaara, "A drone system for autonomous mapping flights inside a forest – a feasibility study and first results," *The International Archives of the Photogrammetry, Remote Sensing and Spatial Information Sciences*, vol. XLVIII-1/W2-2023, pp. 597–603, 2023.
 - [10] V. Karjalainen, N. Koivumäki, T. Hakala, A. George, J. Muhojoki, E. Hyypä, J. Suomalainen, and E. Honkavaara, "Autonomous robotic drone system for mapping forest interiors," *The International Archives of the Photogrammetry, Remote Sensing and Spatial Information Sciences*, vol. XLVIII-2-2024, pp. 167–172, 2024.
 - [11] K. Mohta, K. Sun, S. Liu, M. Watterson, B. Pfrommer, J. Svacha, Y. Mulgaonkar, C. J. Taylor, and V. Kumar, "Experiments in fast, autonomous, gps-denied quadrotor flight," in *2018 IEEE International Conference on Robotics and Automation (ICRA)*, 2018, pp. 7832–7839.
 - [12] X. Liu, G. V. Nardari, F. Cladera, Y. Tao, A. Zhou, T. Donnelly, C. Qu, S. W. Chen, R. A. F. Romero, C. J. Taylor, and V. Kumar, "Large-scale autonomous flight with real-time semantic slam under dense forest canopy," *IEEE Robotics and Automation Letters*, vol. 7, no. 2, pp. 5512–5519, 2022.
 - [13] S. S. Harithas, R. D. Yadav, D. Singh, A. K. Singh, and K. M. Krishna, "CCO-VOXEL: Chance Constrained Optimization over Uncertain Voxel-Grid Representation for Safe Trajectory Planning," in *2022 International Conference on Robotics and Automation (ICRA)*, 2022, pp. 11 087–11 093.
 - [14] Z. Zou, C. Yuan, W. Xu, H. Li, S. Zhou, K. Xue, and F. Zhang, "LTA-OM: Long-term association LiDAR-IMU odometry and mapping," *Journal of Field Robotics*, vol. 41, no. 7, p. 2455 – 2474, 2024.
 - [15] S. W. Chen, G. V. Nardari, E. S. Lee, C. Qu, X. Liu, R. A. F. Romero, and V. Kumar, "Sloam: Semantic lidar odometry and mapping for forest inventory," *IEEE Robotics and Automation Letters*, vol. 5, no. 2, pp. 612–619, 2020.
 - [16] K. Koide, M. Yokozuka, S. Oishi, and A. Banno, "Glim: 3d range-inertial localization and mapping with gpu-accelerated scan matching factors," *Robotics and Autonomous Systems*, vol. 179, p. 104750, 2024.
 - [17] Y. Ren, Y. Cai, F. Zhu, S. Liang, and F. Zhang, "Rog-map: An efficient robocentric occupancy grid map for large-scene and high-resolution lidar-based motion planning," *arXiv preprint arXiv:2302.14819*, 2023.
 - [18] M. Fliess, J. Lévine, P. Martin, and R. Pierre, "Flatness and defect of non-linear systems: introductory theory and examples," *International Journal of Control*, vol. 61, no. 6, pp. 1327–1361, 1995.
 - [19] S. Liu, M. Watterson, K. Mohta, K. Sun, S. Bhattacharya, C. J. Taylor, and V. Kumar, "Planning dynamically feasible trajectories for quadrotors using safe flight corridors in 3-d complex environments," *IEEE Robotics and Automation Letters*, vol. 2, no. 3, pp. 1688–1695, 2017.
 - [20] W. Xu, Y. Cai, D. He, J. Lin, and F. Zhang, "FAST-LIO2: Fast Direct LiDAR-Inertial Odometry," *IEEE Transactions on Robotics*, vol. 38, no. 4, pp. 2053–2073, 2022.
 - [21] C. Yuan, J. Lin, Z. Zou, X. Hong, and F. Zhang, "STD: Stable Triangle Descriptor for 3D place recognition," in *2023 IEEE International Conference on Robotics and Automation (ICRA)*, 2023, pp. 1897–1903.
 - [22] M. Quigley, K. Conley, B. Gerkey, J. Faust, T. Foote, J. Leibs, R. Wheeler, A. Y. Ng *et al.*, "ROS: an open-source Robot Operating System," in *ICRA workshop on open source software*, vol. 3, no. 3.2. Kobe, 2009, p. 5.
 - [23] X. Liang, Y. Wang, J. Pyörälä, M. Lehtomäki, X. Yu, H. Kaartinen, A. Kukko, E. Honkavaara, A. E. Issaoui, O. Nevalainen *et al.*, "Forest in situ observations using unmanned aerial vehicle as an alternative of terrestrial measurements," *Forest ecosystems*, vol. 6, pp. 1–16, 2019.
 - [24] G. Kim, "FAST-LIO-SLAM: FAST-LIO + Scan Context," 2021. [Online]. Available: https://github.com/gisbi-kim/FAST_LIO_SLAM
 - [25] —, "SC-LIO-SAM: Scan Context + LIO-SAM," 2021. [Online]. Available: <https://github.com/gisbi-kim/SC-LIO-SAM>
 - [26] —, "SC-LIO-SAM: Scan Context + LeGO-LOAM," 2021. [Online]. Available: <https://github.com/gisbi-kim/SC-LeGO-LOAM>
 - [27] K. Li, M. Li, and U. D. Hanebeck, "Towards high-performance solid-state-lidar-inertial odometry and mapping," *IEEE Robotics and Automation Letters*, vol. 6, no. 3, pp. 5167–5174, 2021.
 - [28] G. Kim, Y. S. Park, Y. Cho, J. Jeong, and A. Kim, "Mulran: Multimodal range dataset for urban place recognition," in *Proceedings of the IEEE International Conference on Robotics and Automation (ICRA)*, Paris, May 2020.
 - [29] N. Carlevaris-Bianco, A. K. Ushani, and R. M. Eustice, "University of michigan north campus long-term vision and lidar dataset," *The International Journal of Robotics Research*, vol. 35, no. 9, pp. 1023–1035, 2016.
 - [30] A. Karhunen, "Evaluating the applicability of autonomous lidar-based flying algorithms for flying with uncrewed aerial vehicles inside forests," Master's thesis, School of Electrical Engineering, Aalto University, Espoo, Finland, 2024. [Online]. Available: <https://aaltodoc.aalto.fi/items/3da44e19-c72e-4428-b100-3f99b0ac0b89>
 - [31] M. Burri, J. Nikolic, P. Gohl, T. Schneider, J. Rehder, S. Omari, M. W. Achtelik, and R. Siegwart, "The euroc micro aerial vehicle datasets," *The International Journal of Robotics Research*, 2016. [Online]. Available: <http://ijr.sagepub.com/content/early/2016/01/21/0278364915620033.abstract>
 - [32] A. Geiger, P. Lenz, and R. Urtasun, "Are we ready for autonomous driving? the kitti vision benchmark suite," in *Conference on Computer Vision and Pattern Recognition (CVPR)*, 2012.

APPENDIX

A detailed overview of all individual flights conducted for this paper is presented in this section. Tables 4 and 5 present the individual flights done with the original system in medium forest with a target flight velocity of 1 m/s and 2 m/s, respectively. Table 6 presents the individual flights done with the original system in the difficult forest with a target flight velocity of 1 m/s. Tables 7 and 8 present the individual flights done with the optimized system in the medium forest, with a target flight velocity of 1 m/s and 2 m/s, respectively. Tables 9 and 10 present the individual flight done with the optimized system in the difficult forest with a target flight velocity of 1 m/s and 2 m/s, respectively. The failure reasons are presented for failed flights in parentheses under the "Success" column with the following failure meanings: "Tree": collision with a tree, "Leaves": a cloud of leaves thrust from the ground, "NaN": NaNs generated during SFC generation, and "Unstable": unstable flying causing a failure. Point-to-point average speed, average flying speed, and t_{extra} were measured for only successful flights. An "x" indicates that no data was collected.

TABLE 4: Overview of the flights flown with the original system with a target flight velocity of 1 m/s in the medium forest.

Flight	Success	Flight end point	Flight time	Point-to-point average speed	Average flight speed	t_{extra}
1	Yes	(55.96, -0.45, 1.45)	93.5 s	0.62 m/s	0.81 m/s	22.7 s
2	Yes	(58.14, -2.96, 0.83)	102.0 s	0.57	0.68	17.0 s
3	No (Leaves)	(8.76, -0.98, 1.16)	x	x	x	x
4	Yes	(59.45, -2.04, 0.96)	82.0 s	0.73	0.75	2.2 s
5	Yes	(59.54, -1.93, 0.94)	80.1 s	0.74	0.80	6.1 s
6	No (Tree)	(21.76, 0.08, 1.40)	x	x	x	x
7	No (NaN)	(42.13, -1.96, 1.39)	x	x	x	x
8	Yes	(59.54, -2.00, 1.00)	79.3 s	0.75	0.83	7.7 s
9	Yes	(59.97, -2.01, 0.98)	80.3 s	0.75	0.79	4.1 s
10	No (Leaves)	(29.81, -2.13, 1.42)	x	x	x	x
11	Yes	Unknown	≈ 79 s	≈ 0.76	unknown	unknown
12	No (Unstable)	(20.17, 0.32, 1.73)	x	x	x	x
13	Yes	(57.58, -3.02, 0.95)	75.2 s	0.77	0.79	2.0 s
14	Yes	(57.88, -2.89, 0.92)	133.8 s	0.43	0.60	39.5 s
15	Yes	(58.04, -2.79, 0.92)	87.0 s	0.67	0.78	12.6 s

TABLE 5: Overview of the flights flown with the original system with a target flight velocity of 2 m/s in the medium forest.

Flight	Success	Flight end point	Flight time	Point-to-point average speed	Average flight speed	t_{extra}
1	No (Unstable)	(17.22, -0.60, 0.44)	x	x	x	x
2	No (Unstable)	(10.74, 2.75, 0.08)	x	x	x	x
3	No (Unstable)	(12.90, 0.41, 0.42)	x	x	x	x

TABLE 6: Overview of the flights flown with the original system with a target flight velocity of 1 m/s in the difficult forest.

Flight	Success	Flight end point	Flight time	Point-to-point average speed	Average flight speed	t_{extra}
1	Yes	(55.96, -0.45, 1.45)	94.8 s	0.59	0.64	7.9 s
2	Yes	(58.50, 1.38, 0.97)	101.3 s	0.58	0.75	23.4 s
3	No (NaN)	(45.17, -2.58, 0.00)	x	x	x	x
4	Yes	(60.00, -2.74, 0.93)	194.7 s	0.31	0.63	98.3 s
5	No (Tree)	(43.27, -0.35, 0.94)	x	x	x	x
6	Yes	(57.26, -0.95, -0.06)	175.4 s	0.33	0.70	96.1 s
7	No (Unstable)	$\approx (30, 2, 1)$	x	x	x	x
8	Yes	(55.87, -3.70, 1.38)	157.6 s	0.35	0.72	88.1 s
9	No (NaN)	(41.80, 0.21, 1.40)	x	x	x	x
10	No (Unstable)	(44.24, -2.04, 0.01)	x	x	x	x
11	No (Tree)	(34.48, -1.63, 0.35)	x	x	x	x
12	No (NaN)	(29.81, 0.09, 0.16)	x	x	x	x
13	No (Tree)	(34.17, -2.06, 0.24)	x	x	x	x
14	Yes	(63.26, 0.75, -0.16)	142.0 s	0.45	0.76	54.4 s
15	No (NaN)	(48.15, 1.13, 0.37)	x	x	x	x

TABLE 7: Overview of the flights flown with the optimized system with a target flight velocity of 1 m/s in the medium forest.

Flight	Success	Flight end point	Flight time	Point-to-point average speed	Average flight speed	t_{extra}
1	Yes	(60.07, -0.14, 1.04)	75.6	0.79	0.82	2.0 s
2	Yes	(59.98, 0.01, 0.98)	80.2	0.75	0.78	3.7 s
3	No (Leaves)	(11.15, 0.93, 0.00)	x	x	x	x
4	No (Leaves)	(11.31, 0.85, 0.10)	x	x	x	x
5	Yes	(60.00, -0.01, 1.46)	77.4	0.78	0.83	4.8 s
6	Yes	(59.99, -0.02, 1.44)	75.6	0.79	0.84	4.0 s
7	Yes	(60.01, -0.01, 1.45)	76.1	0.79	0.80	0.7 s
8	Yes	(59.86, 0.01, 1.46)	76.8	0.78	0.81	2.8 s
9	Yes	(59.99, -0.02, 1.42)	77.6	0.77	0.79	1.2 s
10	Yes	(60.01, -0.03, 1.47)	77.1	0.78	0.80	1.9 s
11	Yes	(60.13, 0.01, 1.42)	93.1	0.65	0.70	6.6 s
12	No (Leaves)	(35.23, -1.29, 0.77)	x	x	x	x
13	Yes	(60.14, -0.00, 1.48)	76.9	0.78	0.81	3.1 s
14	Yes	(60.10, 0.00, 1.47)	76.8	0.78	0.81	2.5 s
15	Yes	(60.13, -0.03, 1.46)	81.7	0.74	0.78	5.0 s

TABLE 8: Overview of the flights flown with the optimized system with a target flight velocity of 2 m/s in the medium forest.

Flight	Success	Flight end point	Flight time	Point-to-point average speed	Average flight speed	t_{extra}
1	Yes	(59.95, -0.01, 1.47)	39.6	1.51	1.58	1.8 s
2	Yes	(59.97, -0.02, 1.47)	40.4	1.48	1.53	1.2 s
3	Yes	(60.04, -0.01, 1.47)	44.7	1.34	1.44	3.1 s
4	Yes	(59.94, -0.03, 1.46)	40.9	1.46	1.53	1.8 s
5	Yes	(59.93, 0.01, 1.52)	49.4	1.21	1.45	8.0 s
6	Yes	(59.96, -0.01, 1.53)	41.7	1.44	1.53	2.5 s
7	No (Leaves)	(34.15, 0.57, 0.91)	x	x	x	x
8	Yes	(59.98, -0.02, 1.48)	43.5	1.38	1.54	4.5 s
9	No (Leaves)	(16.45, 4.10, 0.34)	x	x	x	x
10	No (Unstable)	(59.94, -0.42, 0.43)	x	x	x	x
11	Yes	(60.02, 0.04, 1.52)	42.3	1.42	1.54	3.3 s
12	Yes	(59.97, 0.03, 1.58)	47.4	1.26	1.46	6.3 s
13	Yes	(59.93, 0.03, 1.58)	51.7	1.16	1.42	9.5 s
14	Yes	(59.97, 0.06, 1.51)	42.1	1.42	1.53	2.8 s
15	Yes	(60.08, 0.04, 1.51)	52.8	1.14	1.23	3.9 s

TABLE 9: Overview of the flights flown with the optimized system with a target flight velocity of 1 m/s in the difficult forest.

Flight	Success	Flight end point	Flight time	Point-to-point average speed	Average flight speed	t_{extra}
1	Yes	$\approx (55.2, 0.14, 0.93)$	76.6	≈ 0.72	≈ 0.78	≈ 6.5 s
2	Yes	(55.91, 0.33, 0.15)	86.2	0.65	0.74	11.6 s
3	Yes	(56.37, -0.26, 0.37)	79.2	0.71	0.77	5.9 s
4	Yes	(55.86, -0.10, 0.45)	81.6	0.68	0.78	10.7 s
5	Yes	(55.64, 0.20, 0.57)	78.3	0.71	0.76	6.0 s
6	Yes	(58.59, 1.40, 0.91)	115.9	0.51	0.62	22.6 s
7	Yes	(55.95, 1.61, 0.04)	82.7	0.68	0.76	9.9 s
8	Yes	(58.61, 1.45, 0.93)	91.8	0.64	0.76	14.6 s
9	Yes	(55.49, -0.55, 1.19)	80.9	0.69	0.77	4.0 s
10	Yes	(56.63, -1.42, 0.87)	82.9	0.68	0.77	9.6 s
11	Yes	(54.74, -0.40, 0.14)	79.6	0.69	0.77	5.6 s
12	Yes	(55.66, -0.18, 0.02)	77.7	0.72	0.78	6.6 s
13	Yes	(58.60, 1.33, 0.96)	80.0	0.73	0.79	6.0 s
14	Yes	(58.54, 1.40, 0.93)	107.3	0.55	0.65	17.1 s
15	Yes	(58.95, 1.05, 0.93)	96.6	0.61	0.72	15.3 s

TABLE 10: Overview of the flights flown with the optimized system with a target flight velocity of 2 m/s in the difficult forest.

Flight	Success	Flight end point	Flight time	Point-to-point average speed	Average flight speed	t_{extra}
1	No (Leaves)	(11.52, 1.05, 0.01)	x	x	x	x
2	Yes	(60.63, -0.03, 0.94)	64.3	0.94	1.17	12.5 s
3	No (Unstable)	(22.71, -1.50, 0.12)	x	x	x	x
4	No (Leaves)	(29.91, -0.23, 0.00)	x	x	x	x
5	No (Leaves)	(53.07, -0.08, 0.01)	x	x	x	x
6	No (Tree)	(14.89, -1.02, 0.63)	x	x	x	x
7	No (Unstable)	(28.47, 1.55, 0.09)	x	x	x	x
8	No (Tree)	(27.25, 0.92, 0.01)	x	x	x	x
9	Yes	(55.15, -0.46, 0.63)	49.3	1.12	1.38	10.2 s
10	No (Unstable)	(28.27, 0.36, 0.28)	x	x	x	x
11	Yes	(56.51, -1.06, 1.04)	52.3	1.08	1.45	14.0 s
12	No (Leaves)	(30.43, -0.32, 0.22)	x	x	x	x
13	No (Leaves)	(47.83, -2.19, 0.10)	x	x	x	x
14	Yes	(56.60, 1.20, 0.99)	42.0	1.35	1.56	6.0 s
15	Yes	(59.99, -0.46, 1.01)	76.1	0.79	1.06	19.3 s